Healing of confined polymer films following deformation at high shear rate

Yingxi Zhu and Steve Granick[a)]

Department of Materials Science and Engineering, University of Illinois, Urbana, Illinois 61801

(Received 1 March 2000; final revision received 23 May 2000)

Synopsis

Recovery of equilibrated linear viscoelastic response of confined polymer melts, following cessation of large-amplitude shear in a surface forces apparatus, was found to be a single exponential process. The most extensive experiments concerned a polydimethylsiloxane of narrow molecular weight distribution and weight-average molecular weight $M_w = 8330\ g\ mol^{-1}$, for which recovery times were in the range 2–12 h when the film thickness (D) was $D/R_G = 0.5–6$ (R_G is radius of gyration). Initially, to produce the deformed state, the films were sheared with effective shear rate $\approx 10^4\ s^{-1}$. Recovery was probed by the subsequent application of small-amplitude sinusoidal shear forces at 256 Hz. Surprisingly, the nonlinear and linear shear moduli evaluated at the input frequency nearly coincided just before and just after cessation of large-amplitude shear. Recovery time constants, τ_R, increased linearly with the prior shear rate at a given thickness (D). But at a given shear rate and variable D, τ_R passed through a *maximum* at $D/R_G \approx 3.5$; thinner films recovered more quickly. This contrasts with relaxation times in films that were at rest prior to shear. Due to slip, these thinner films ($D/R_G < 3.5$) may have been less uniformly deformed than thicker ones. We conjecture that chains in very thin films were separated by large-amplitude shear into two distinct populations, each moving preferentially with each of the sliding surfaces. Recovery kinetics would then reflect interdiffusion during which chain configurations lose memory of the distinction between top and bottom surfaces. © *2000 The Society of Rheology.* [S0148-6055(00)00305-9]

I. INTRODUCTION

Tribologists and rheologists are interested in studying the structure and dynamics of confined polymer films whose thickness is comparable to molecular dimensions. Both computer simulations [Thompson and Robbins (1990); Thompson, Grest, and Robbins (1992); Bhushan, Israelachvili, and Landman (1995)] and experiments show that relaxation times of confined liquid films are enormously prolonged relative to these same films in the bulk state. On the experimental side, polysiloxanes comprise a frequently studied model system [Horn *et al.* (1989); Van Alsten and Granick (1990); Israelachvili *et al.* (1990); Hu and Granick (1992); Granick and Hu (1994); Peanasky *et al.* (1994); Hirz *et al.* (1996)]. At laboratory frequencies, these films are commonly more elastic than viscous in response to small-amplitude deformation; when molecularly thin, they appear to ''solidify.'' The emphasis in this field [Bhushan *et al.* (1995)] has been on the transition from ''stick'' to ''slip,'' from a small deformation to a large one.

[a)]Author to whom correspondence should be addressed. Electronic mail: sgranick@uiuc.edu

This study concerns the reverse process: recovery of the originally undeformed linear viscoelastic response following cessation of a large-amplitude oscillatory shear. Our goal was to quantify how recovery depends on prior shear deformation amplitude, film thickness, and the molecular weight of linear chains. Stress relaxation after cessation of steady-state shear flow has been studied previously, with regard to concern bulk samples and it is common to observe long-lived recovery [Stratton and Bucher (1973); Ferry (1980); Bousmina *et al.* (1998); Qiu and Bousmina (1999)]. Transient behavior is also observed when polymer oligomers are confined between solid surfaces to a thickness comparable to molecular dimensions. For example, when sliding velocity is changed from one level to another, stress continues to adjust even after hundreds of seconds [Peanasky (1995); Dhinojwala *et al.* (1996)]. If rapid flow is resumed, the level of static friction depends on the waiting time before flow was reinitiated [Yoshizawa and Israelachvili (1993)]. This slow equilibration has been interpreted in terms of the rearrangement of molecules after they deform and lose some interpenetration upon the imposition of high shear forces.

The recovery to the originally undeformed state after relatively ''easy'' sliding at high shear rate can be studied and is especially convenient when dealing with films of near-molecular thickness. Then, it is easy to produce large effective shear rates because even a small absolute velocity amounts to a large shear rate when normalized by a smaller film thickness). Furthermore, it is possible, using piezoelectric instrumentation, to also produce deformations small enough to produce a linear viscoelastic response in these same systems. In the present study, elapsed time was the primary variable. What happens to confined polymers when shear sliding with large deformation stops? How long does the healing process take? What influences the rate of healing?

These questions are relevant to tribology, to the deformation of colloids coated with polymers, and to the deformation of polymer matrices containing filler particles.

II. EXPERIMENT

The investigation was performed using a surface force apparatus [Israelachvili (1992)] modified with a device for dynamic oscillatory shear [Van Alsten and Granick (1988); Peachey *et al.* (1991)]. The surfaces, two thin sheets of freshly cleaved muscovite mica, were silvered on one side and then glued onto fused silica lenses of cylindrical shape, with the silvered side down using symdiphenylcarbazide. This chemical was first melted for the gluing process, then quenched rapidly. The assembly was mounted in the surface forces instrument in a crossed-cylinder geometry so that simple asperity contact could be produced.

Separation of the two opposed mica surfaces was measured using multiple beam interferometry between the silver coatings on the back sides of the mica sheets by comparing the calibrated thickness of the mica sheets in the absence of intervening liquid, with the larger thickness measured in the presence of liquid. The mica surfaces were smoothly curved when the normal pressure was small. However in most of these experiments the sheets were deformed by normal pressure and produced a flattened geometry at the apex of the crossed cylinders, which amounted to a parallel-plate configuration. Optical interferometry was then used to measure the area of the flattened spots, and shear forces were normalized by contact area to allow the calculation of effective shear moduli [Peachey *et al.* (1991)].

The polydimethylsiloxane (PDMS) oligomers were purchased from Polymer Source, Inc. (Montréal, Canada). Their characteristics are summarized in Table I. Most extensively investigated was the hydroxyl capped PDMS with an weight-average molecular

TABLE I. PDMS oligomer characteristics.

Sample	M_w (g mol^{-1})	M_w/M_n	End functionality	R_G (Å)
PDMS 8 K	8330	1.10	–OH	25
PDMS 6 K	6750	1.01	$-CH_3$	22
PDMS 2 K	2200	1.09	$-CH_3$	11
PDMS 0.75 K	750	1.19	$-CH_3$	6

weight of 8330 g mol^{-1}; other samples were of lower molecular weight, as low as 750 g mol^{-1}. All were used without further purification.

A drop of the polymer melts was inserted into the gap between the mica surfaces with a glass pipette cleaned in a manner described elsewhere [Granick and Hu (1994)]. Throughout the experiments, the chamber of the surface forces instrument was kept dry by exposing the atmosphere to an excess of P_2O_5, which is extremely hygroscopic. The experiments commenced 1 h after injecting the drop. All the experiments were conducted at $25 \pm 0.2\,^{\circ}C$, which is approximately 100 °C above the bulk glass transition temperature.

The shear device is described in detail elsewhere [Peachey *et al.* (1991); Granick and Hu (1994)]. The upper surface was mounted onto a rigid boat supported by two pieces of piezoelectric bimorphs, attached with leaf springs, one on each side of the boat. A periodic voltage was applied to one of the bimorphs, causing it to deflect. Thus, the upper surface sheared the liquid of interest back and forth over the lower surface. The amplitude and phase of voltage induced at the input frequency in the other piezolectric bimorph, which was mounted symmetrically, were detected using a lock-in amplifier (Stanford Research Systems model 850 DSP). The effective in-phase and out-of-phase responses can be calculated in the traditional ways from the amplitude attenuation and phase shift [Ferry (1980)] thus affording a measure of the energy stored and dissipated during a cycle of deformation.

When experiments concern parallel plates of area A separated by distance D, the shear storage modulus (G') and loss modulus (G'') at a frequency (ω) can be related to the spring constant (k_L) and dashpot coefficient (b_L) of the liquid (L) by the geometry of the rheometer,

$$G'_{\text{eff}} = (D/A)k_L\,, \tag{1}$$

$$G''_{\text{eff}} = (D/A)\omega b_L\,. \tag{2}$$

This parallel-plate geometry was produced when the compressive force was large enough to flatten the mica cylinders at their apex. The resulting circular contact, measured directly by optical interferometry, generally had diameter in the range of 10–30 μm, and the normal pressures in this case are considered to be the normal force divided by the measured area of contact. The accuracy in the measurement of the contact diameter was ± 5 μm. In fact, it should be recognized that there exists a distribution of pressure within such a contact circle, as discussed in standard textbooks. It is well known that if adhesive forces are small compared to external forces, the classical equations for Hertzian (nonadhesive) contact apply. Then the pressure is zero at the circle periphery and is (3/2)(mean pressure) at the center. Flattened contact was observed by eye starting at a normal force of ≈ 2 mN m^{-1}.

Recognizing the intrinsic inhomogeneity of an interfacial structure, we refer in Eqs. (1) and (2) to *effective* shear moduli, G_{eff}; Eqs. (1) and (2) present a convenient method by which to normalize force measurements. In the discussion below we will sometimes omit the subscript for convenience and simplicity.

When the compressive force was too low to flatten the mica sheets, one deals with smoothly curved crossed cylinders. In these instances, in order to normalize the force by an effective area of contact (A_{eff}), we used the Langbein approximation [Israelachvili (1992)],

$$A_{\text{eff}} = 2\pi RH \quad (R \gg D), \tag{3}$$

where R is the mean radius of curvature of the crossed cylinders and h is the surface separation. Experimental evidence that supported this estimate of the effective contact area was presented previously [Peanasky *et al.* (1994)]. Then the measured in-phase and out-of-phase viscoelastic responses could be normalized by the effective area, A_{eff}, allowing estimates of the conventional storage and loss moduli between parallel plates. We have also presented elsewhere an alternative normalization based on the Hertz theory for nonadhesive contact between adhesive bodies [Demirel and Granick (1998)].

The experiments were performed at a fixed frequency of 256 Hz. First, the films were deformed for 30 min at a constant shear rate by applying force impulses using triangular voltage wave forms from a function generator (Hewlett Packard model 3325A). Next, the time-dependent nonequilibrium surface structure was probed by the subsequent application of small-amplitude sinusoidal shear. In the first stage the applied voltage was varied from 0.8 to 3.3 V root-mean square (rms) and in the second stage it was constant at 0.05 V rms. The repetitive applications of force impulses and oscillations as well as the measurements of response were all controlled by computer. A novel aspect of the present experiment is that the forcing function, comprised of a triangular (rather than sinusoidal) force wave form, should have produced a constant shear rate during each half period of oscillation. It is of course interesting to ask how responses might differ if the shear direction were never reversed. Such an experiment would probably require a device involving rotating shear; to date, all surface-force and atomic force microscopy (AFM) experiments of which we are aware have involved periodic deformations.

As this device operates, there is some compliance in the device itself and some in the sample of interest. This serial combination, in parallel with the complex impedance of the piezoelectric bimorphs themselves, constitutes the mechanical circuit by which we model the device [Granick and Hu (1994); Reiter *et al.* (1994)]. In this model, the force applied to this parallel combination is split according to the ratio of the complex impedance. Here $Z = k + i\omega b$, k is the real part of Z (the spring constant), ω is the radian frequency, and b is the (dissipative) dashpot coefficient. Denoting applied force by the symbol F, this gives

$$F = (|Z_D + Z_S|)\Delta x_{\text{tot}}, \tag{4}$$

where Z_D and Z_S are the complex impedances for the device (mainly the bimorphs) and the serial combination of glue and the sample, respectively, and Δx_{tot} is the total deflection of the receiver bimorph, equal to the deflection of the serial combination of glue and the confined liquid.

The compliance of the apparatus (Fig. 1) is calibrated by bringing the top and bottom dry mica surfaces into direct contact. The deformability of this ''glue'' in series with the confined film is accounted for [Reiter *et al.* (1994)] by

$$\Delta x_L = \Delta x_{\text{tot}} |Z_G/(Z_G + Z_L)|. \tag{5}$$

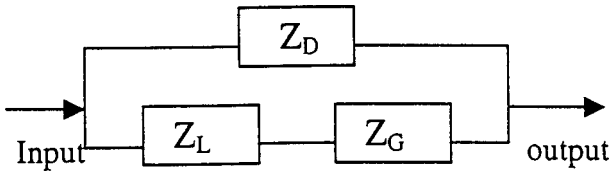

FIG. 1. Sketch of the mechanical model used to analyze the data. Contributions from the device and a serial combination of glue layers and liquid are parallel. The symbols Z_D, Z_G, and Z_L are the complex impedances of the device, glue layers, and liquid, respectively. The complex impedance of each element can be represented by a parallel arrangement of elastic and dissipative subelements.

Here Δx_L is the actual deflection within the confined liquid film and Z_G and Z_L are the complex impedances representing the glue layers and the confined liquid, respectively. We have found from experience that this compliance does not change during an experiment; it takes the same value, in a given experiment, regardless of the contact spot and experimental run.

This analysis allows one to correct the raw data for apparatus compliance. Because of the parallel arrangement of the device, the force applied to the system (device, liquid, and glue) is not the same as the force applied to the confined liquid film.

III. RESULTS

For reference, the force-distance profile of the PDMS 8 K is shown in Fig. 2. Plotted against film thickness is the force in the normal direction ($F_\perp$) required to compress the film to a given film thickness (D), normalized by the mean radius of curvature of the mica sheets (R). Care was taken to wait long enough for equilibration at each film thickness, in many cases up to 20–30 min. These findings are consistent with others

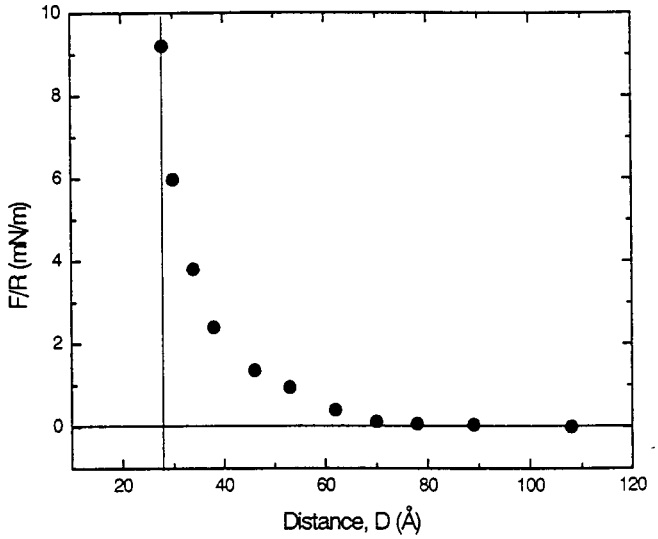

FIG. 2. Force-distance profile of PDMS 8 K with $M_w = 8330\ \mathrm{g\,mol^{-1}}$. Force ($F$) required to produce deformation to a given film thickness (D), normalized by the mean radius of curvature of the mica sheets (R) is plotted against film thickness. Care was taken to wait, in many cases for up to 20 min, to achieve equilibration at each film thickness. The vertical line denotes a ''hard wall,'' a minimal thickness that did not change with increasing compressive force.

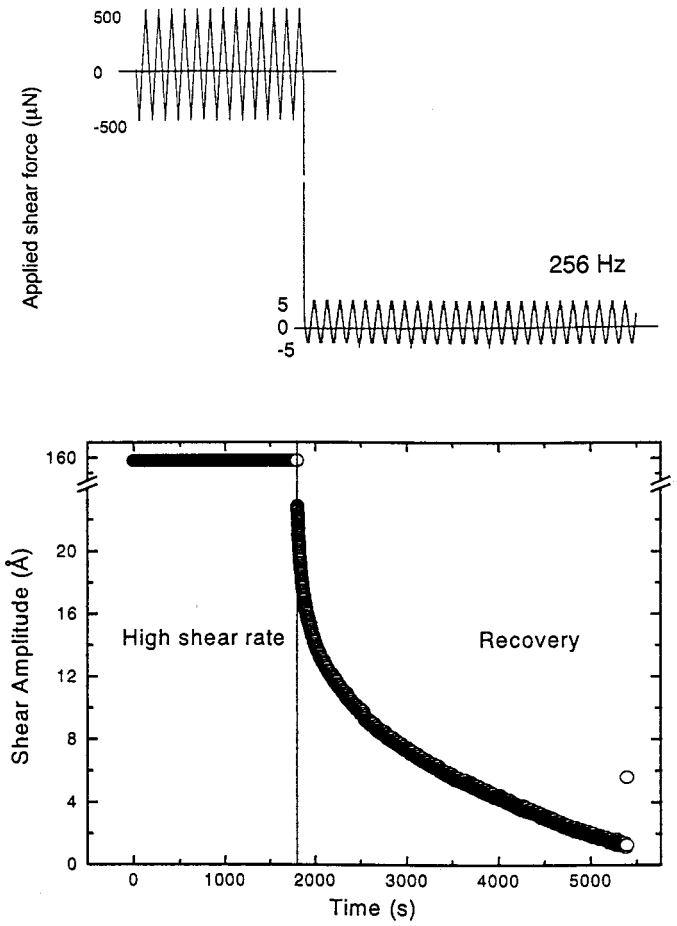

FIG. 3. First the PDMS with $M_w = 8330\ \mathrm{g\ mol^{-1}}$ and thickness 68 Å was deformed at large amplitude for 30 min using a triangular-shaped voltage wave form at 256 Hz. The force amplitude was 500 μN, resulting in rms amplitude during shear of 144 Å, which is several times larger than the characteristic size of an ideal PDMS coil in the melt state. Then the forcing function was suddenly switched to a gentle sinusoidal oscillation of 5 μN amplitude at the same frequency. Top: Schematic illustration of the experiment. Bottom: Deformation amplitude is plotted against elapsed time. Following cessation of large-amplitude shear, this deformation decreased monotically with time elapsed, reflecting progressive stiffening of the confined film. The film thickness was 68 Å. The vertical line denotes the time when large-amplitude shear was stopped.

previously reported in the literature [Horn *et al.* (1989)]. It is worth noting that static shear forces began, on our experimental time scale, starting at $D/R_G \approx 2$ (as specified in Table I, R_G is the estimated radius of gyration of the polymer in the undeformed melt state). However anomalous shear responses were observed at film thickness $D/R_G \approx 6$—much larger than the range of static forces.

A typical shear experiment involving PDMS 8 K is shown in Fig. 3. Seeking to deform the polymer at constant speed, rather than at a continuously variable shear rate as in our previous studies that employed large-amplitude sinusoidal deformation [see, for example, Granick, Hu, and Carson (1994)], the sample was deformed using a *triangular*-shaped voltage wave form. The force amplitude was large, 500 μN, resulting in large

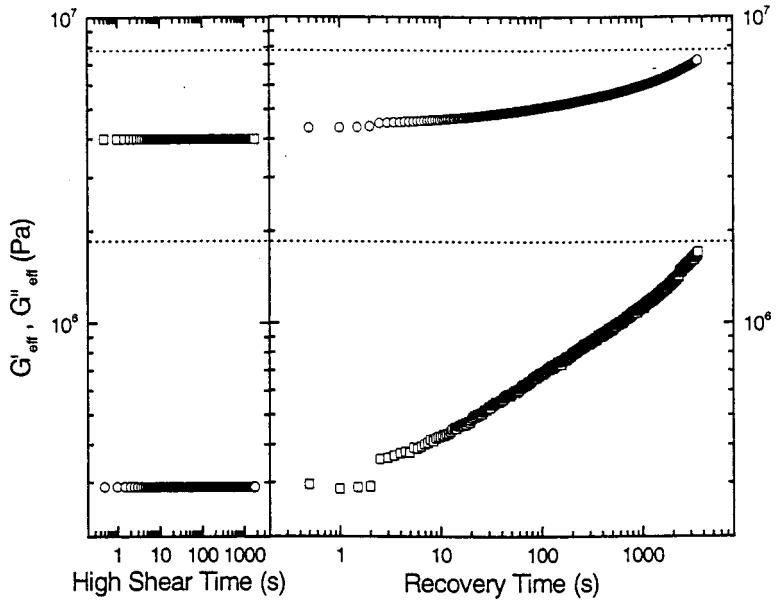

FIG. 4. Same experiment as that in Fig. 3 but analyzed concerning changes of the elastic and viscous effective shear moduli, G' (squares) and G''(circles), respectively. These are plotted on log–log scales as a function of time elapsed after cessation of large-amplitude shear. The data points are the size of the 5% error bar. The vertical line denotes the time when large-amplitude shear ceased. Dotted horizontal lines denote levels of the effective shear moduli of the originally undeformed sample.

effective shear rates and consequently in highly nonlinear responses of the confined PDMS. The rms amplitude during shear was 144 Å, which is considerably greater than R_G.

This deformation at high shear rate was continued for 30 min in order to ensure a steady state. Then the forcing function was suddenly switched to a gentle sinusoidal oscillation of 5 μN force amplitude at the same frequency. The resulting deformation amplitude decreased: at first rapidly, followed by slower decay. This reflected the progressive stiffening of the confined film. The healing process persisted for several house and appeared only asymptotically to approach the response of the originally undeformed sample.

Parenthetically, we emphasize that the measurement did not really measure compliance (as one might at first suppose). This is because the actual force applied to the sample decreased, the stiffer the sample, as shown by the model presented in Fig. 1. The force applied to the measuring system (apparatus, sample, and glue) was split into the parallel combination of the mechanical impedances of the forcer (Z_D) and the serial combination of the latter two (Z_S). The spring constants of the sample (in phase and out of phase with the drive) were obtained after correcting for instrumental compliance (see Sec. II). Normalizing by film thickness and contact area, the effective storage and loss moduli, G'_{eff} and G''_{eff}, were calculated.

Figure 4 plots, on a log–log scale, time-dependent changes of the elastic and viscous moduli. One notices a predominantly viscous response throughout, i.e., $G''_{\text{eff}} > G'_{\text{eff}}$. Both moduli decreased substantially upon the application of large-amplitude shear (the elastic modulus more strongly so than the viscous component). During the healing pro-

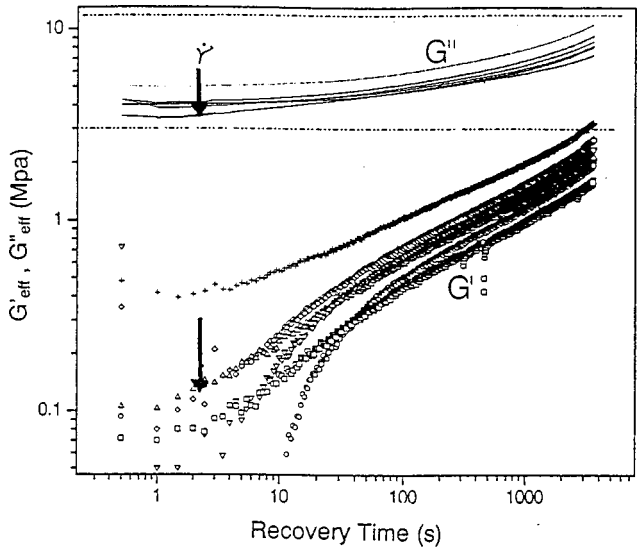

FIG. 5. Healing kinetics of the viscoelastic shear moduli after four different amplitudes of large-amplitude shear. The data concern the PDMS with $M_w = 8330\ \mathrm{g\ mol^{-1}}$ and thickness of 68 Å. The elastic modulus G' (symbols) and loss moduli G'' (lines) are plotted on log–log scales against time elapsed after cessation of large-amplitude shear. The prior driving force amplitudes were 75 (circles), 120 (squares), 300 (triangles), 375 (inverted triangles), 400 (diamonds), and 500 μN (crosses), respectively. The order of increasing force amplitude, shown by the vertical arrows, corresponds to effective shear rates in the range of 7×10^3–$2.2\times10^4\ \mathrm{s^{-1}}$ (cf. Fig. 7). Dotted horizontal lines denote levels of the effective shear moduli before large-amplitude shear.

cess, after cessation of large-amplitude shear, they recovered only slowly towards their earlier unperturbed values.

Of course, the effective moduli measured during large-amplitude shear represented only the fundamental component of a response that also contained numerous higher odd-order components. The physical meaning of these nonlinear viscoelastic functions has been discussed by Matsumoto and co-workers, who showed that the energy dissipated over one complete cycle of periodic deformation is determined solely by G'' evaluated at the fundamental frequency [Matsumoto *et al.* (1973)], although higher-order harmonics are required to describe the time-dependent energy dissipated during any given cycle of periodic deformation. For molecularly thin films, we have examined this point elsewhere from an experimental point of view [Granick *et al.* (1994)].

It is fascinating to notice, in Fig. 4, that the linear viscoelastic loss modulus evaluated immediately following cessation of large-amplitude shear was numerically almost identical to that measured during shear at the fundamental frequency. This is unexpected *a priori* [Matsumoto *et al.* (1973)] but lends suggestive empirical support in favor of analyzing nonlinear G'' evaluated at the fundamental frequency.

Recovery after five other driving force amplitudes was also investigated for comparison. The time-dependent storage and loss moduli against elapsed time are plotted in Fig. 5 log–log scales. The data from these multiple experiments (quantitative analysis is presented below) confirm the patterns suggested by the single experiment summarized in Fig. 4.

Seeking to quantify the recovery process, we experimented with various functional forms. We were not successful in finding a simple relation that depended on the absolute value of the time-dependent moduli, but the time-dependent *deviations* from the unperturbed moduli seemed a more fundamental quantity. In Fig. 6, for the data shown in Fig.

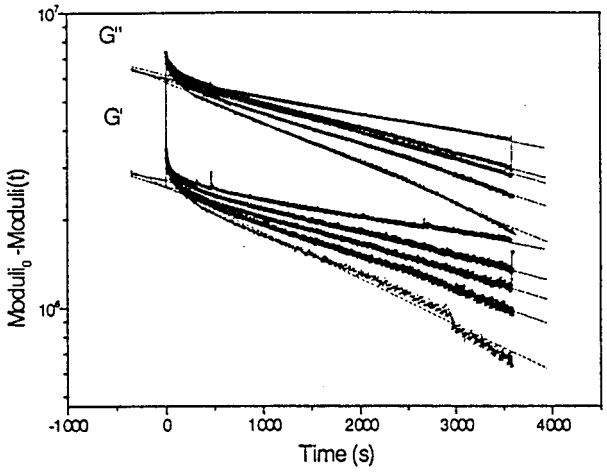

FIG. 6. Deviations of G' and G'' are plotted semilogarithmically against elapsed time for the same data as those shown in Fig. 5. After an initial period of relatively rapid recovery, the data suggest a single recovery time, τ_R.

3, these deviations in $G'(t)$ and $G''(t)$ are plotted semilogarithmically against elapsed time. Apart from a faster recovery period during the earliest times when limited data were available, the data suggest a single exponential recovery process.

No dependence was found on the duration of large-amplitude shear before its cessation. The durations tested, 5 min, 15 min, and 1 h, gave the same results as these presented above. The recovery curves coincided, within experimental uncertainty, with those in Fig. 4. It appeared that once large-amplitude shear forces acted on these confined films, equilibration to the steady-state nonequilibrium response was rapid on these time scales.

The amplitude of large-amplitude shear, tested by varying the drive force by a factor of nearly 7, from 75 to 500 μN (30 min duration in every case) did not alter the qualitative recovery phenomenon but did influence the recovery time. It is convenient to define the effective shear rate as $\dot{\gamma} = \omega\gamma$, the product of shear frequency and shear strain (shear deformation normalized by film thickness). In Fig. 7, the recovery time constants for G'' and G' are each plotted separately against the prior effective shear rate. Recovery time increased with increasing shear rate during the initial deformation.

The linearity of this dependence over the tested range of shear rate is striking. The data, however, extrapolate to zero shear rate at a finite ordinate, which is not physically realistic, signifying that the linear dependence must break down when the shear rate is lower than was tested in these experiments. It is reasonable to suppose that the higher shear rates caused the molecules in these films to be more strongly deformed and therefore to require more time to recover to the undeformed state. Reasons for linear dependence over the tested range of shear rate are not understood at present, but the phenomenon might afford a useful interpolation method.

Knowing from prior studies that the linear viscoelastic spectrum of confined polymer melts slows down monotonically with diminishing film thickness [Hu and Granick (1992); Granick and Hu (1994); Demirel and Granick (1996)], it was interesting to compare the dependence on film thickness (D) in the present experiment. In Fig. 8, recovery times are plotted against normalized film thickness after prior deformation at

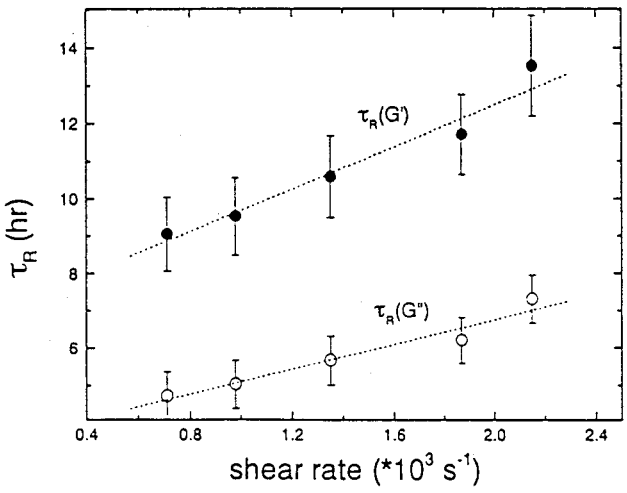

FIG. 7. Recovery times τ_R of G' and G'' plotted against the effective shear rate during the prior large-amplitude shear for the same data as those shown in Fig. 5.

three large shear rates; the qualitative pattern was the same. The film thickness has been normalized by $R_G \approx 25$ Å estimated for PDMS of this molecular weight in the bulk melt state [Edwards *et al.* (1983)].

As a function of film thickness, τ_R for G' was immeasurably fast until the onset of static forces resisting compression. It subsequently increased with diminishing film thickness, then passed through a *maximum.* Finally, at the highest compression beyond which compression to thinner films was not possible (15 Å) a slight increase was observed. The

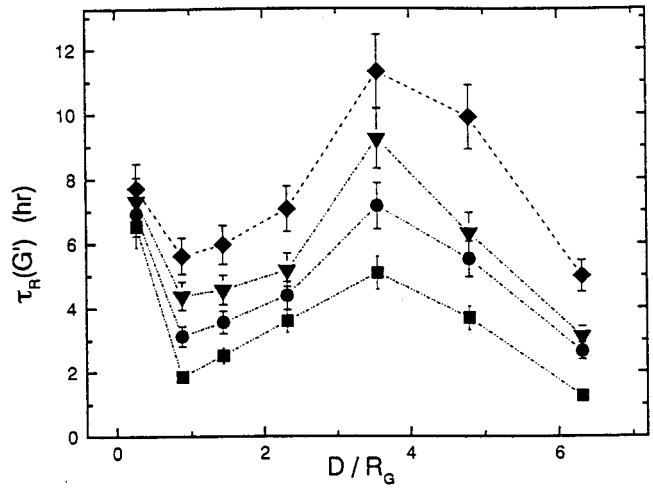

FIG. 8. Recovery times τ_R of G' plotted against film thickness normalized by the estimated radius of gyration, $R_G = 25$ Å, for the PDMS with $M_w = 8330\ \mathrm{g\,mol^{-1}}$. Each curve denotes a different prior shear rate in the range of 750–2400 $\mathrm{s^{-1}}$. In some cases, in order to make the comparison at the same shear rate, the data were interpolated using the linear relationship established in Fig. 7.

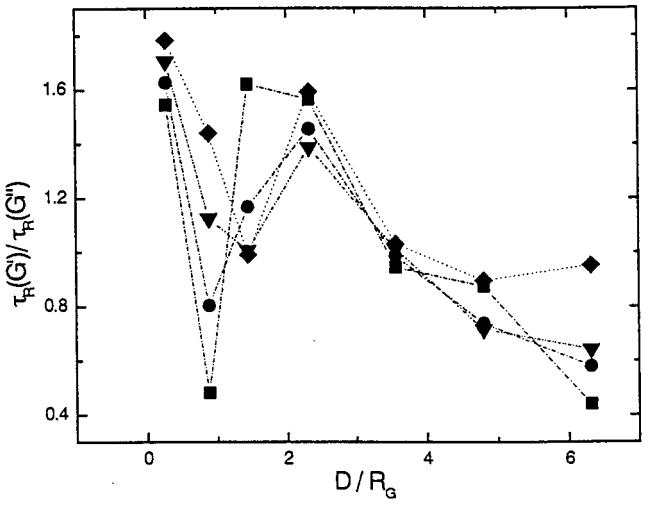

FIG. 9. For the same experiments as those shown in Fig. 9, the ratio of the recovery time for the two viscoelastic moduli, $\tau_R(G')/\tau_R(G'')$, is plotted against film thickness normalized by the estimated radius of gyration, $R_G = 25$ Å.

decrease suggested the possibility that large-amplitude shear deformation was increasingly inhomogeneous as the film thickness decreased.

The recovery times of G'' followed the same trend. The ratio, $\tau_R(G')/\tau_R(G'')$, is plotted in Fig. 9 against the normalized film thickness, D/R_G. Differences in this ratio are not large, but the differences relative to unity are striking. When $D/R_G > 1$ (a relatively large thickness), the viscous component recovered most rapidly. For the thinner films, in which $D/R_G < 1$, the elastic component recovered most rapidly.

A brief investigation was made of the dependence on molecular weight. As described in Table I, PDMS samples of four different molecular weights, $M_w = 750$, 2220, 6750, and 8310 g mol^{-1}, were chosen for study. In order to induce similar deformation by the same driving shear forces in 30 min, the comparisons were made at approximately the same D/R_G, $D/R_G \approx 1.90$. (The R_G are enumerated in Table I and the exact values of D are specified in the caption of Fig. 10.) The results concerning the recovery times of G' and G'' are shown in Fig. 10, where recovery time is plotted as a function of molecular weight. From these findings, no definitive conclusion is possible concerning the question of whether the healing process depended on molecular weight. The dilemma originates partly from the limited range of molecular weight used in this investigation. Moreover, further work is needed to decide whether comparison at the same D/R_G constitutes a correct comparison of data involving samples of different molecular weight.

Finally, comparison was made to other systems of confined chain molecules. Apart from PDMS, confined films were studied of poly(phenylmethysiloxane) (PPMS) with $M_w = 2140$ g mol^{-1} [Hu and Granick (1992)], a perfluoropolyether (Demnum) with $M_w = 2200$ g mol^{-1} [Cho and Granick (1996)], and squalane, an alkane 24 carbon units long with 6 pendant methyl groups, $C_{30}H_{62}$ [Reiter *et al.* (1994)]. Findings concerning PMMS were very similar results to those with PDMS. However, in confined films of Demnum and squalane, recovery from large deformation was complete after a few seconds; the recovery process was too rapid to measure on the available time scale. These

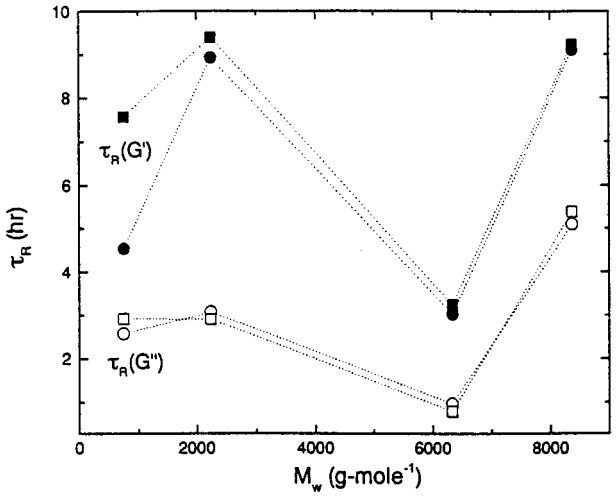

FIG. 10. Recovery times [squares denote $\tau_R(G'')$, circles denote $\tau_R(G')$] plotted against molecular weight at film thickness $D/R_G \approx 1.9$ for four PDMS samples differing in molecular weight by a factor of 10. The measured values of D during these experiments involving four PDMS samples (M_w = 750, 2220, 6750, and 8310 g mol^{-1}) were 11, 21, 42, and 49 Å, corresponding in each case to $D/R_G \approx 1.9$.

differences from the polysiloxane systems are not understood but may be related to different intensities with which chain segments adsorb to the mica surfaces.

IV. DISCUSSION AND CONCLUSIONS

Healing processes evidently follow a different time scale than the motions characteristic of a sample that starts out at rest; the recovery kinetics presented in this article contrast strongly with the picture that emerged from studying confined films whose initial state was at rest [Hu and Granick (1992); Bhushan *et al.* (1995); Demirel and Granick (1996)]. In those instances it was found that films stiffen when confined between adsorbing surfaces: the thinner the film, the stiffer the viscoelastic responses and the longer the terminal relaxation time. In this study we found, in contrast, that the recovery time constant changed relatively little as the film thickness was varied from 6 to 0.5 R_G. It actually passed through a weak maximum. There is no contradiction with prior experiments; these healing experiments constitute, to the best of our knowledge, the first of their kind.

This physical problem is surely linked to strong adsorption of polymer segments to the opposed solid surfaces. Indeed, in other experiments where polymer melts were confined between nonadsorbing surfaces, the equilibrated surface force-distance profile was found to be zero down to a very small thickness ($\approx$ four segmental dimensions) regardless of molecular weight, and enhanced effective shear moduli were not observed when the film thickness was larger [Peanasky *et al.* (1994)]. We expect that if the polymer in the present study were confined between nonadsorbing surfaces, the remarkably slow recovery times described here would no longer be observed. Slip would then take place at the solid–fluid interface rather than within the fluid itself, and the recovery time would reflect relatively rapid diffusion associated with re-establishing intimate contact with the solid wall after the cessation of shear. The comparison with other chain molecules of

different chemical makeup—squalane, Demnum, and phenylmethylsiloxane—further suggests that these kinetics are connected to adsorption. It is reasonable to conclude that the more rapid kinetics observed in those systems are connected to weaker sticking energy (as well as to possible differences in molecular packing in the confined state).

The exceptional length of these recovery times is worth emphasizing: they were hours long, although the experiments concerned oligomers of relatively low molecular weight. This suggests that molecular origins of the recovery process should not be sought in Brownian motion that concerns center-of-mass motions of entire molecules (although the molecular structure of the interfacial film was certainly deformed by the strong shear). In seeking to make this picture more specific, two limiting cases can be imagined: (a) molecular conformations of all molecules were deformed (so that all molecules must participate in a recovery process); and (b) molecular conformations were perturbed only at some kind of slip plane.

The thickest films in these experiments recovered most rapidly, of course; in the bulk state, the oligomer chains studied here display very low viscosity [Ferry (1980)].

When solids bearing chains adsorbed from the melt are brought progressively closer together, one expects these surface-bound layers to progressively interdigitate and intertwine and this results in progressive retardation of the linear viscoelastic response [Hu and Granick (1992); Granick and Hu (1994)]. It seems reasonable to conjecture that, when these surface-bound layers first intertwine (but not extensively so), chains throughout the sample will be deformed by strong shear. But ultrathin films of even small molecules are known to undergo wall slip [Thompson and Robbins (1990); Thompson, Grest, and Robbins (1992); Bhushan *et al.* (1995)] such that shear is localized to one portion of the film. This occurs at the solid surface if the film is nonadsorbing or within the film itself if the surface is strongly attractive. We expect this situation to hold progressively more strongly as thickness diminishes. If so, chain deformations may become progressively more localized to the portion of the sample near to the slip interface.

Based on these considerations, we speculate that kinetics of the healing process may involve the following mechanism. In an equilibrated system at rest, there can be no differentiation between the top and bottom of the confined sample; the molecular conformations are distributed without preference. But the interface must separate into two portions in the event of slip: one portion moves preferentially with the top surface and the other preferentially with the bottom one. This scenario suggests the hypothesis that recovery responses reflected diffusion: the interdiffusion of two initially distinct sheared layers. The absence of a clearcut dependence on molecular weight suggests that very local motions of the chains must be responsible, not center-of-mass diffusion. Related arguments have been proposed previously concerning viscoelastic healing of bulk samples [Qiu and Bousmina (1999)], although center-of-mass diffusion was invoked with regard to those systems. Direct rheo-optical measurements of chain–chain motions and relaxations will be needed to test the interdiffusion hypothesis directly at a molecular level.

ACKNOWLEDGMENTS

The authors thank A. Ostling for setting up the initial experiments and performing the healing experiment with polyphenylmethylsiloxane. They also appreciate financial support from the taxpayers of United States via a grant from the National Science Foundation (Tribology Program).

References

Bhushan, B., J. N. Israelachvili, and U. Landman, ''Nanotribology—Friction, wear and lubrication at the atomic scale,'' Nature (London) **374**, 607–616 (1995).

Bousmina, M., H. Qiu, M. Grmela, and G. E. Klemberg-Sapieha, ''Diffusion at polymer/polymer interfaces probed by rheological tools,'' Macromolecules **31**, 8273–8280 (1988).

Cho, Y.-K. and S. Granick, ''Shear of confined perfluorinated molecules: Effect of side branching,'' Wear **200**, 346–352 (1996).

Demirel, A. L. and S. Granick, ''Glass-like transition of a simple confined fluid,'' Phys. Rev. Lett. **77**, 2261–2264 (1996).

Demirel, A. L. and S. Granick, ''Transition from static to kinetic friction in a model lubricated system,'' J. Chem. Phys. **109**, 6889–6897 (1998).

Dhinojwala, A., L. L. Cai, and S. Granick, ''Critique of the friction coefficient concept in wet (lubricated) sliding,'' Langmuir **12**, 4537–4542 (1996).

Edwards, C. J. C., D. Rigby, R. F. T. Stepto, K. Dodgson, and J. A. Semlyen, ''Studies of cyclic and linear polydimethylsiloxanes: 10. Calculations of radii of gyration,'' Polymer **24**, 391–399 (1983).

Ferry, J. D., *Viscoelastic Properties of Polymers*, 3rd ed. (Wiley, New York, 1980).

Granick, S. and H.-W. Hu, ''Nanorheology of confined polymer melts. 1. Linear shear response at strongly adsorbing surfaces,'' Langmuir **10**, 3857–3866 (1994).

Granick, S., H.-W. Hu, and G. A. Carson, ''Nanorheology of confined polymer melts. 2. Nonlinear shear response at strongly adsorbing surfaces,'' Langmuir **10**, 3867–3873 (1994).

Hirz, S., A. Subbotin, C. Frank, and G. Hadziioannou, ''Static and kinetic friction of strongly confined polymer films under shear,'' Macromolecules **29**, 3970–3974 (1996).

Horn, R. G., S. J. Hirz, G. Hadziioannou, C. W. Frank, and J. M. Catala, ''A reevaluation of forces measured across thin polymer films—Nonequilibrium and pinning effects,'' J. Chem. Phys. **90**, 6767–6774 (1989).

Hu, H.-W. and S. Granick, ''Viscoelastic dynamics of confined polymer melts,'' Science **258**, 1339–1342 (1992).

Israelachvili, J., *Intermolecular and Surface Forces* (Wiley, New York, 1992).

Joshe, Y. M., A. K. Lele, and R. A. Mashelkar, ''Slipping fluids: A unified transient network model,'' J. Non-Newtonian Fluid Mech. **89**, 303–335 (2000).

Matsumoto, T., Y. Segawa, Y. Warashina, and S. Onogi, ''Nonlinear behavior of viscoelastic materials. II. The method of analysis and temperature dependence of nonlinear viscoelastic functions,'' Trans. Soc. Rheol. **17**, 47–62 (1973).

Peachey, J., J. Van Alsten, and S. Granick, ''Design of an apparatus to measure the shear response of ultrathin liquid films,'' Rev. Sci. Instrum. **62**, 463–473 (1991).

Peanasky, J., ''Structure and dynamics of confined chain molecules,'' Ph.D. thesis, University of Illinois at Urbana–Champaign, 1995.

Peanasky, J., L. L. Cai, S. Granick, and C. R. Kessel, ''Nanorheology of confined polymer melts. 3. Weakly adsorbing surfaces,'' Langmuir **10**, 3874–3879 (1994).

Qui, H. and M. Bousmina, ''New technique allowing the quantification of diffusion at polymer polymer interfaces using rheological analysis: Theoretical and experimental results,'' J. Rheol. **43**, 551–568 (1999).

Reiter, G., A. L. Demirel, J. Peanasky, L. L. Cai, and S. Granick, ''Stick to slip transition and adhesion of lubricated surfaces in moving contact,'' J. Chem. Phys. **101**, 2606–2615 (1994).

Thompson, P. A., G. S. Grest, and M. O. Robbins, ''Phase transitions and universal dynamics in confined fluids,'' Phys. Rev. Lett. **68**, 3448–3451 (1992).

Thompson, P. A., M. O. Robbins, and G. S. Grest, ''Structure and shear response in nanometer-thick films,'' Isr. J. Chem. **35**, 93–106 (1995).

Van Alsten, J. and S. Granick, ''Molecular tribometry of ultrathin liquid films,'' Phys. Rev. Lett. **61**, 2570–2573 (1988).

Yoshizawa, H. and J. Israelachvili, ''Fundamental mechanisms of interfacial friction. 2. Stick-slip friction of spherical and chain molecules,'' J. Phys. Chem. **97**, 11300–11313 (1993).